Full-Wave Analysis of Circular Microstrip Resonators in Multilayered Media Containing Uniaxial Anisotropic Dielectrics, Magnetized Ferrites, and Chiral Materials

Vicente Losada, Rafael R. Boix, *Member, IEEE*, and Manuel Horno, *Member, IEEE*

***Abstract*—In this paper, Galerkin's method in the Hankel transform domain is applied to the determination of the resonant frequencies, quality factors, and radiation patterns of circular microstrip patch resonators. The metallic patches are assumed to be embedded in a multilayered substrate, which may contain uniaxial anisotropic dielectrics, magnetized ferrites, and/or chiral materials. The numerical results obtained show that important errors can be made in the computation of the resonant frequencies of the resonators when substrate dielectric anisotropy, substrate magnetic anisotropy and/or substrate chirality are ignored. Also, it is shown that the resonant frequencies of circular microstrip resonators on magnetized ferrites can be tuned over a wide frequency range by varying the applied bias magnetic field. Finally, the computed results show that the resonance and radiation properties of a circular microstrip patch on a chiral material is very similar to those of a circular patch of the same size printed on a nonchiral material of lower permittivity.**

***Index Terms*—Complex media, microwave planar circuits, microstrip patches, resonators.**

I. Introduction

CIRCULAR microstrip patch resonators can be used either as antennas [1] or as components of oscillators and filters in microwave integrated circuits (MIC's) [2]. Since the bandwidth of microstrip patch resonators around their operating resonant frequencies is very narrow [2], it is important to develop accurate algorithms for the computation of those resonant frequencies.

Multilayered media have proven to have an application as substrates of MIC's and printed circuit antennas (PCA's). For instance, concerning microstrip antennas, one superstrate (radome) placed on top of a microstrip patch antenna can be used for protecting that antenna against environmental hazards, such as rain, fog, and snow [3]. When a superstrate is placed on top of a patch antenna, the resonant frequency of the antenna is shifted and this shift may take the antenna out of its original operating frequency band [3]. Therefore, an algorithm for the computation of the resonant frequencies of microstrip patches should be able to account for multilayered substrate effects.

Apart from multilayered media, in the last few years, some interest has arisen on studying how the performance of MIC's and PCA's is affected when complex materials—e.g., anisotropic dielectrics, magnetized ferrites, chiral materials, etc.—are used as substrates of those circuits and antennas. Thus, bearing in mind that some of the standard materials used as substrates of printed microwave circuits and antennas exhibit dielectric anisotropy [4], Pozar has shown that substrate dielectric anisotropy should always be taken into account when designing microstrip patch antennas because if anisotropy were ignored, the antennas might operate out of the expected frequency band [5]. Magnetized ferrites belong to the class of complex materials that have proven to have potential application as substrates of MIC's and PCA's. For instance, measurements have shown that the resonant frequencies of microstrip antennas printed on ferrite substrates can be varied over a wide frequency range by adjusting the bias magnetic field [6]. Apart from that, ferrite substrates can be used for reducing the radar cross section of microstrip antennas [7], [8] and for achieving circularly polarized microstrip antennas with a single feed [9]. Also, it should be pointed out that when ferrite materials are used as substrates of microstrip phased arrays, a considerable improvement in the "impedance-matching versus scan angle" performance is achieved [9], [10]. Very recently, some attention has also been paid to the possibility of using chiral materials [11] as substrates of MIC's and PCA's. Pozar [12] has stated that there are serious disadvantages to using chiral materials as substrates of microstrip antennas because of increased losses due to surface-wave excitation and high cross-pol levels. However, Toscano and Vegni [13] have recently shown that chiral substrates can be advantageously employed for increasing the directivity and the small bandwidth of microstrip antennas. These two latter results indicate that the performance of microstrip antennas on chiral substrates still has to be studied more thoroughly.

In this paper, the authors apply Galerkin's method in the Hankel transform domain (HTD) [14]–[16] to the full-wave computation of the resonant frequencies, quality factors, and

Manuscript received March 2, 2000. This work was supported by the Comisión Interministerial de Ciencia y Tecnología, Spain under Project TIC98–0630.

V. Losada is with the Microwaves Group, Department of Applied Physics, Escuela Universitaria de Ingeniería Tecnica Agrícola, University of Seville, 41013 Seville, Spain.

R. R. Boix is with the Microwaves Group, Department of Electronics and Electromagnetism, School of Physics, University of Seville, 41012 Seville, Spain.

M. Horno, deceased, was with the Microwaves Group, Department of Electronics and Electromagnetism, School of Physics, University of Seville, 41012 Seville, Spain.

Publisher Item Identifier S 0018-9480(00)04672-X.

radiation patterns of the resonant modes of circular microstrip patch resonators in the case in which the metallic patches are embedded in multilayered media, which may contain uniaxial anisotropic dielectrics, magnetized ferrites, and chiral materials. Since there are abundant results for the behavior of microstrip resonators of rectangular geometry on anisotropic dielectrics [2], [17]–[20], in this paper, just a few original results will be presented for microstrip resonators of circular geometry on anisotropic dielectrics. Concerning the topic of microstrip resonators on magnetized ferrites, although this topic has already been treated by several researchers [20]–[22], these researchers have not considered phenomena such as the existence of a cutoff frequency region for the resonant frequencies of microstrip resonators on magnetized ferrites, which will be addressed in detail in this paper. Aside from the effect of anisotropic materials on microstrip resonators, this paper will also show that microstrip resonators printed on chiral substrates tend to behave as microstrip resonators printed on nonchiral substrates of lower permittivity. In Section II, the application of Galerkin's method in the HTD to the analysis of the circular microstrip resonators is described. In Section III, results are presented for the resonant frequencies, quality factors, and radiation patterns of circular microstrip resonators on substrates of the different types treated in this paper. Finally, conclusions are summarized in Section IV.

II. Formulation of the Problem and Numerical Method

Fig. 1(a) and (b) shows the side and top views of a circular microstrip patch of radius a embedded in a multilayered medium. The electromagnetic fields existing inside this resonant structure are assumed to show a time dependence of the type $e^{j\omega t}$ (where ω is complex to account for radiation losses), which will be suppressed throughout. Both the circular metallic patch and the ground plane of Fig. 1 are assumed to be perfect electric conductors (PEC's) of neglecting thickness. The layers of the substrate are assumed to be of infinite extent along the x and y coordinates, and these layers are also assumed to be made of any of the three following materials:

1) uniaxial anisotropic dielectrics;
2) magnetized ferrites with applied bias magnetic field;
3) chiral materials.

In case the ith layer of the multilayered substrate $(i = 1, \cdots, N)$ is a uniaxial anisotropic dielectric, its optical axis will be assumed to be the z-axis [4]. For that case, the permeability of the anisotropic dielectric will be taken as μ_0 and the permittivity tensor will be taken as [5]

$$\bar{\epsilon}_i = \epsilon_0 \begin{pmatrix} \epsilon_t^i & 0 & 0 \\ 0 & \epsilon_t^i & 0 \\ 0 & 0 & \epsilon_z^i \end{pmatrix}. \tag{1}$$

In case the ith layer of the substrate $(i = 1, \cdots, N)$ is a magnetized ferrite, it will be assumed that the bias magnetic field of the ferrite is directed along the z-axis. For that case, the permittivity of the ferrite material will be taken as $\epsilon_0 \epsilon_f^i$ and the permeability tensor will be taken as [9]

$$\bar{\mu}_i = \mu_0 \begin{pmatrix} \mu^i & j\kappa^i & 0 \\ -j\kappa^i & \mu^i & 0 \\ 0 & 0 & 1 \end{pmatrix}. \tag{2}$$

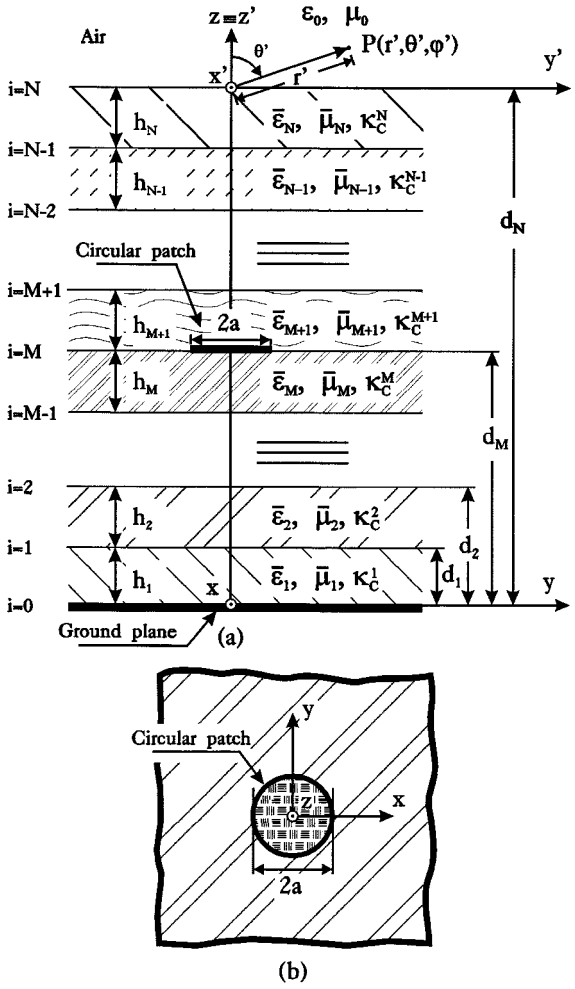

Fig. 1. (a) Side and (b) top views of a circular microstrip patch embedded in a multilayered medium that may contain uniaxial anisotropic dielectrics, magnetized ferrites, and chiral materials.

Throughout this paper, ferrite materials will be assumed to be magnetically saturated. Under this assumption, the elements of the permeability tensor of (2), $\bar{\mu}_i$, can be obtained in terms of the gyromagnetic ratio $\gamma = 1.759 \cdot 10^{11}$ C/kg, the saturation magnetization of the ferrite material M_s^i, the internal bias magnetic field H_0^i, and the linewidth ΔH^i, as explained in [23].

Finally, in case the ith layer of the substrate of Fig. 1 $(i = 1, \cdots, N)$ is a chiral material, this material will be assumed to be both chiral and reciprocal (i.e., it will be a Pasteur medium according to [11]) with permittivity $\epsilon_0 \epsilon_c^i$, permeability $\mu_0 \mu_c^i$, and dimensionless chiral parameter κ_c^i. Inside this material, the constitutive relations among the four vector quantities $\mathbf{D}$, $\mathbf{B}$, $\mathbf{E}$, and $\mathbf{H}$ will be given by [11]

$$\mathbf{D} = \epsilon_0 \epsilon_c^i \mathbf{E} - j\kappa_c^i \sqrt{\epsilon_0 \mu_0}\, \mathbf{H} \tag{3}$$

$$\mathbf{B} = \mu_0 \mu_c^i \mathbf{H} + j\kappa_c^i \sqrt{\epsilon_0 \mu_0}\, \mathbf{E}. \tag{4}$$

Under resonant conditions, let $\mathbf{j}_M(\rho, \phi) = j_{M,\rho}(\rho, \phi)\hat{\boldsymbol{\rho}} + j_{M,\phi}(\rho, \phi)\hat{\boldsymbol{\phi}}$ and $\mathbf{E}_t(\rho, \phi, z = d_M) = E_\rho(\rho, \phi, z = d_M)\hat{\boldsymbol{\rho}} + E_\phi(\rho, \phi, z = d_M)\hat{\boldsymbol{\phi}}$ be the expressions of both the current density on the patch of Fig. 1 and the transverse electric field at the

plane of the patch, respectively, when cylindrical coordinates are used ($x = \rho\cos\phi$ and $y = \rho\sin\phi$). Owing to the revolution symmetry of the multilayered medium of Fig. 1 around the z-axis, when the Helmholtz equations for the axial field components E_z and H_z are solved in cylindrical coordinates inside each of the layers of that medium, it turns out that the dependence of E_z and H_z on the ϕ coordinate is of the type $e^{jm\phi}$ ($m = \cdots, -2, -1, 0, 1, 2, \cdots$) and, as a consequence of this fact, the dependence of $\mathbf{j}_M(\rho, \phi)$ and $\mathbf{E}_t(\rho, \phi, z = d_M)$ on the ϕ coordinate is also of the type $e^{jm\phi}$. This implies that $\mathbf{j}_M(\rho, \phi)$ and $\mathbf{E}_t(\rho, \phi, z = d_M)$ can both be written as follows:

$$\mathbf{j}_M(\rho,\phi) = \left(j^m_{M,\rho}(\rho)\hat{\boldsymbol{\rho}} + j^m_{M,\phi}(\rho)\hat{\boldsymbol{\phi}}\right)e^{jm\phi}, \quad m = \cdots, -2, -1, 0, 1, 2, \cdots \tag{5}$$

$$\mathbf{E}_t(\rho,\phi,z=d_M) = \left(E^m_{M,\rho}(\rho)\hat{\boldsymbol{\rho}} + E^m_{M,\phi}(\rho)\hat{\boldsymbol{\phi}}\right)e^{jm\phi}, \quad m = \cdots, -2, -1, 0, 1, 2, \cdots. \tag{6}$$

By virtue of (5) and (6), it is possible to follow a mathematical reasoning completely parallel to that shown in [24, eqs. (1)–(14)] for obtaining a relation between $\mathbf{j}_M(\rho, \phi)$ and $\mathbf{E}_t(\rho, \phi, z = d_M)$ in the spectral domain given by (see [24, eq. (13)])

$$\tilde{\mathbf{E}}^H_{M,m}(k_\rho) = \overline{\tilde{\mathbf{G}}}^H_{M,M}(k_\rho)\cdot\tilde{\mathbf{j}}^H_{M,m}(k_\rho), \quad m = \cdots, -2, -1, 0, 1, 2, \cdots \tag{7}$$

where $\tilde{\mathbf{j}}^H_{M,m}(k_\rho)$ and $\tilde{\mathbf{E}}^H_{M,m}(k_\rho)$ are vector functions that have to be determined in terms of the $(m+1)$th and $(m-1)$th Hankel transforms of $j^m_{M,\rho}(\rho, \phi)$, $j^m_{M,\phi}(\rho, \phi)$, $E^m_{M,\rho}(\rho)$, and $E^m_{M,\phi}(\rho)$ as follows:

$$\tilde{\mathbf{j}}^H_{M,m}(k_\rho) = \int_0^\infty \begin{bmatrix} \left(j^m_{M,\rho}(\rho) + jj^m_{M,\phi}(\rho)\right)J_{m+1}(k_\rho\rho) \\ \left(j^m_{M,\rho}(\rho) - jj^m_{M,\phi}(\rho)\right)J_{m-1}(k_\rho\rho) \end{bmatrix}\rho\, d\rho, \quad m = \cdots, -2, -1, 0, 1, 2, \cdots \tag{8}$$

$$\tilde{\mathbf{E}}^H_{M,m}(k_\rho) = \int_0^\infty \begin{bmatrix} \left(E^m_{M,\rho}(\rho) + jE^m_{M,\phi}(\rho)\right)J_{m+1}(k_\rho\rho) \\ \left(E^m_{M,\rho}(\rho) - jE^m_{M,\phi}(\rho)\right)J_{m-1}(k_\rho\rho) \end{bmatrix}\rho\, d\rho, \quad m = \cdots, -2, -1, 0, 1, 2, \cdots \tag{9}$$

In (7), $\overline{\tilde{\mathbf{G}}}^H_{M,M}(k_\rho)$ stands for a 2×2 matrix, which plays the role of a dyadic Green's function in the HTD [24]. This dyadic Green's function in the HTD can be obtained in a straightforward way in terms of the two-dimensional Fourier transform (TDFT) of the dyadic Green's function of the multilayered medium of Fig. 1 (see [24, eqs. (9) and (14)]), which, in turn, can be determined by using a recurrent algorithm obtained via the equivalent boundary method [25].

Once (7) has been obtained, Galerkin's method in the HTD can be applied to that equation in order to determine the resonant frequencies and quality factors of the resonant modes of the circular microstrip patch of Fig. 1. After following the process described in [24, eqs. (15)–(22)], a nonlinear eigenvalue equation for the operating angular frequency ω is obtained. The solutions of this nonlinear equation provide the necessary information for obtaining the resonant frequencies and quality factors of the resonant modes of the structure of Fig. 1. In fact, let $\omega_{mn} = 2\pi(f^{mn}_r + jf^{mn}_i)$ ($m = \cdots, -2, -1, 0, 1, 2, \cdots; n = 1, 2, 3, \cdots$) be the set of complex roots of the aforementioned nonlinear equation. In that case, the quantities f^{mn}_r ($m = \cdots, -1, 0, 1, \cdots; n = 1, 2, 3, \cdots$) stand for the resonant frequencies of the circular microstrip patch and the quantities $Q_{mn} = f^{mn}_r/2f^{mn}_i$ ($m = \cdots, -1, 0, 1, \cdots$; $n = 1, 2, 3, \cdots$) stand for the quality factors [2].

Once f^{mn}_r and Q_{mn} are known for a particular resonant mode of the structure of Fig. 1, one can derive expressions for the vector functions $\mathbf{j}_M(\rho, \phi)$ and $\tilde{\mathbf{j}}^H_{M,m}(k_\rho)$ corresponding to that particular resonant mode. The vector function $\tilde{\mathbf{j}}^H_{M,m}(k_\rho)$ can then be used for computing the radiation electric field $\mathbf{E}(r', \theta', \phi')$ in the air upper half-space of Fig. 1 ($\{r', \theta', \phi'\}$ is a local set of spherical coordinates defined in Fig. 1) by means of the stationary phase method (see [26, pp. 164–169] and [24, eqs. (23) and (24)]).

The basis functions chosen in this paper for approximating the current density on the circular patch of Fig. 1 [see (5)] have different expressions for axial–symmetric resonant modes ($m = 0$) [14] and for nonaxial-symmetric resonant modes ($m \neq 0$) [15]. In the case of axial-symmetric modes, the basis functions chosen for $j^0_{M,\rho}(\rho)$ and $j^0_{M,\phi}(\rho)$ are given by

$$j^0_{M,\rho,i}(\rho) = U_{2i-1}(\rho/a)\sqrt{1-(\rho/a)^2}, \quad i = 1, \cdots, N \tag{10}$$

$$j^0_{M,\phi,i}(\rho) = j\frac{T_{2i-2}(\rho/a)}{\sqrt{1-(\rho/a)^2}}(\rho/a), \quad i = 1, \cdots, N+1 \tag{11}$$

where $U_{2i-1}(\cdot)$ $(i = 1, \cdots, N)$ and $T_{2i-2}(\cdot)$ $(i = 1, \cdots, N+1)$ stand for Chebyshev polynomials of the second and first kinds, respectively.

For nonaxial-symmetric modes, the basis functions chosen for approximating $j^m_{M,\rho}(\rho)$ and $j^m_{M,\phi}(\rho)$ when $m \neq 0$ (see (5)) are given by

$$j^m_{M,\rho,i}(\rho) = U_{2i-1}(\rho/a)\sqrt{1-(\rho/a)^2}\,(\rho/a)^{|m|-2}, \quad m = \cdots, -2-1, 1, 2, \cdots; i = 1, \cdots, N \tag{12}$$

$$j^m_{M,\phi,i}(\rho) = j\frac{T_{2i-2}(\rho/a)}{\sqrt{1-(\rho/a)^2}}(\rho/a)^{|m|-1}, \quad m = \cdots, -2, -1, 1, 2, \cdots; i = 1, \cdots, N+1. \tag{13}$$

The basis functions of (10)–(13) are very similar to the basis functions of [24, eqs. (25)–(28)]. However, whereas $j^0_{M,\phi}(\rho)$ is taken to be zero in [24], $j^0_{M,\phi}(\rho) \neq 0$ in this paper. In order to explain this, it should be noted that when the multilayered medium of Fig. 1 is made of isotropic (and/or anisotropic) dielectrics, the dominant axial-symmetric modes are TM_z ($H_z = 0$) modes

[14] and, as a consequence of this, the azimuthal component of the current density on the patch are zero for these modes ($j^0_{M,\phi}(\rho) = 0$). However, when the multilayered medium contains either ferrite layers or chiral layers, all axial-symmetric modes are hybrid modes ($H_z \neq 0$ and $E_z \neq 0$) and, therefore, the two components of the current density on the patch in these modes turn out to be different from zero ($j^0_{M,\rho} \neq 0$ and $j^0_{M,\phi} \neq 0$).

In [24], the authors demonstrated that the basis functions of the type shown in (10) and (13) are very appropriate for the HTD analysis of microstrip patches embedded in multilayered isotropic dielectric substrates. That is because they ensure a quick convergence of Galerkin's method in the HTD with respect to the number of basis functions, their Hankel transforms can be obtained in closed form in terms of spherical Bessel functions (see [24, Appendix B]), and they lead to HTD infinite integrals, which are amenable to asymptotic analytical integration techniques (see [24, Sec. IV and Appendix C]). Fortunately, all these advantages are kept when the aforementioned basis functions are used in the HTD analysis of circular patches fabricated on anisotropic dielectrics, magnetized ferrites, and/or chiral materials (see Section III for details).

III. Numerical Results

In order to check the validity of the method described in Section II, our results for the resonant frequencies, quality factors, and radiation patterns of the first resonant modes of circular microstrip patches on isotropic dielectric substrates have been compared with previously published results [2], [14], [16] and with measurements. Good agreement has been found in all cases (see [24, Figs. 3–6] for more details).

In Table I, the convergence of the numerical method described in Section II is checked with respect to the number of basis functions (of the type shown in (10)–(13)) used in the approximation of the current density. Results are presented for several resonant modes of circular microstrip patches printed on different materials (one anisotropic dielectric, one magnetized ferrite, and one chiral material). It can be noticed that seven basis functions suffice to obtain the resonant frequencies and quality factors within five significant figures when the substrate is either an anisotropic dielectric or a magnetized ferrite, and within four significant figures when the substrate is a chiral material. Since a small number of basis functions provides very accurate results for the resonant frequencies and quality factors in all the cases studied in Table I, it seems that the basis functions of (10)–(13) are very appropriate for approximating the surface current density on circular microstrip patches fabricated on any kind of substrate. It should be pointed out that whereas the results shown in Table I for the resonant frequencies and quality factors of the circular patches on anisotropic dielectric and chiral material are all for modes in which $m \geq 0$, the results for the circular patch on magnetized ferrite include values of resonant frequencies and quality factors for the mode $m = -1$. In order to explain this, it should be said that whereas in those cases in which the multilayered substrate of Fig. 1 only contains anisotropic dielectrics and/or chiral materials, the resonant frequencies and quality factors of the resonant modes have been found to verify that $f_r^{mn} = f_r^{-m,n}$ and $Q_{mn} = Q_{-m,n}$; in the cases in which magnetized ferrites are allowed to be a part of the multilayered substrate, the authors have found that $f_r^{mn} \neq f_r^{-m,n}$ and $Q_{mn} \neq Q_{-m,n}$. This latter behavior is attributed to the nonreciprocal character of ferrite materials and it is predicted by the cavity model of a circular patch printed on a ferrite substrate [9], [23].

TABLE I
Convergence Pattern of the Resonant Frequencies and Quality Factors of Several Resonant Modes of a Circular Microstrip Patch on Different Substrates with Respect to the Number of Basis Functions Used in the Approximation of the Current Density. In all Tables $a = 5$ mm and $h = 1.27$ mm. Substrates: (a) Uniaxial Anisotropic Dielectric ($\epsilon_t = 5.12, \epsilon_z = 3.4$). (b) Magnetized Ferrite ($\epsilon_f = 15, \mu_0 M_s = 0.065$ T, $\mu_0 H_0 = 0.1$ T, $\mu_0 \Delta H = 0.004$ T). (c) Chiral Material ($\epsilon_c = 4, \mu_c = 1, \kappa_c = 1.5$)

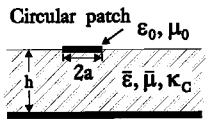

Mode	$m=1, n=1$		$m=2, n=1$		Mode	$m=0, n=1$	
$2N+1$	f_r^{11} (GHz)	Q_{11}	f_r^{21} (GHz)	Q_{21}	N	f_r^{01} (GHz)	Q_{01}
3	8.4034	18.200	14.001	19.159	1	16.548	7.1403
5	8.3403	18.835	13.984	19.253	2	16.254	8.3574
7	8.3400	18.839	13.984	19.261	3	16.251	8.3801
9	8.3400	18.839	13.984	19.261	4	16.251	8.3802

(a)

Mode	$m=1, n=1$		$m=-1, n=1$		$m=0, n=1$	
$2N+1$	f_r^{11} (GHz)	Q_{11}	f_r^{-11} (GHz)	Q_{-11}	f_r^{01} (GHz)	Q_{01}
3	4.3482	48.853	6.0700	70.147	9.1396	71.320
5	4.3368	48.317	6.0201	70.981	8.8473	93.693
7	4.3368	48.317	6.0197	70.999	8.8422	94.276
9	4.3368	48.317	6.0197	70.999	8.8422	94.278

(b)

Mode	$m=1, n=1$		$m=2, n=1$		$m=0, n=1$	
$2N+1$	f_r^{11} (GHz)	Q_{11}	f_r^{21} (GHz)	Q_{21}	f_r^{01} (GHz)	Q_{01}
3	10.712	11.859	16.905	10.915	20.078	6.8962
5	10.763	11.809	16.971	10.753	19.964	7.4296
7	10.763	11.830	16.978	10.753	19.956	7.4874
9	10.764	11.833	16.981	10.749	19.959	7.4884

(c)

In Fig. 2, results are presented for the resonant frequencies of the fundamental mode of circular microstrip patches printed on different anisotropic dielectric substrates and covered by anisotropic dielectric superstrates in such a way that the material of the superstrate always coincides with that of the substrate. In this figure, the results obtained for every patch placed between two anisotropic dielectric layers are compared with the results that would be obtained if the dielectric anisotropy of the layers were neglected and the layers were assumed to be isotropic. The differences between the results obtained considering dielectric anisotropy and the results obtained neglecting dielectric anisotropy reach 4.5% when the anisotropic dielectric is sapphire, 6% when the dielectric is Epsilam-10, and 10% when the dielectric is boron nitride. The authors have also obtained results (not plotted in the current paper) for the circular patches analyzed in Fig. 2 in the case in which the anisotropic dielectric superstrates are not present (i.e., $h_2 = 0$ in Fig. 2). In this latter case, the differences existing between

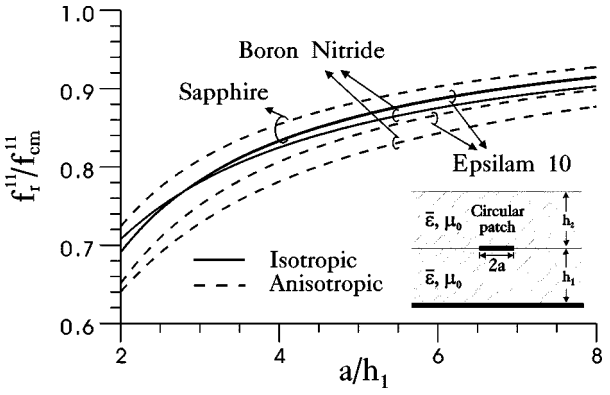

Fig. 2. Normalized resonant frequencies of the fundamental mode ($m = 1$, $n = 1$) of circular microstrip patches printed on an anisotropic dielectric layer with an anisotropic dielectric superstrate of the same type ($h_1 = 0.635$ mm, $h_2 = h_1$, sapphire: $\epsilon_t = 9.4$ and $\epsilon_z = 11.6$, epsilam-10: $\epsilon_t = 13$ and $\epsilon_z = 10.3$, boron nitride: $\epsilon_t = 5.12$ and $\epsilon_z = 3.4$). The normalization factor $f_{cm}^{11} = 1.841/2\pi a\sqrt{\epsilon_0\epsilon_z\mu_0}$ is taken as the resonant frequency that would be obtained in each case by means of the cavity model. The results obtained for the patches on anisotropic dielectrics (dashed lines) are compared with the results obtained for patches on isotropic dielectrics of permittivity $\epsilon_0\epsilon_z$ (solid lines).

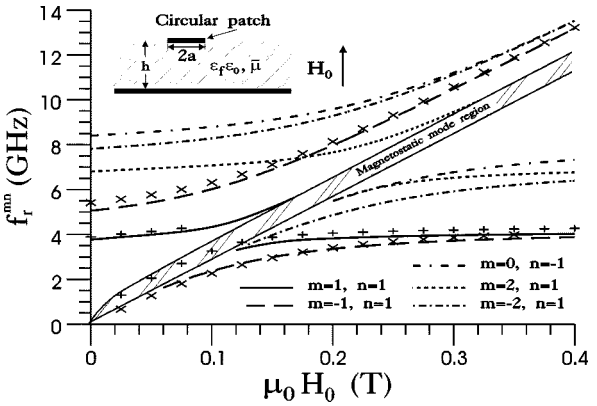

Fig. 3. Resonant frequencies of the first five resonant modes of a circular microstrip patch on a magnetized ferrite versus bias magnetic field ($h = 1.27$ mm, $a = 5$ mm, $\epsilon_f = 15$, $\mu_0 M_s = 0.065$ T, $\mu_0\Delta H = 0$ T). Galerkin's method results for the first two resonant modes (solid lines: $m = 1$, $n = 1$, dashed lines: $m = -1$, $n = 1$) are compared with results obtained for these two modes by means of the cavity model (+: $m = 1$, $n = 1$, ×: $m = -1$, $n = 1$).

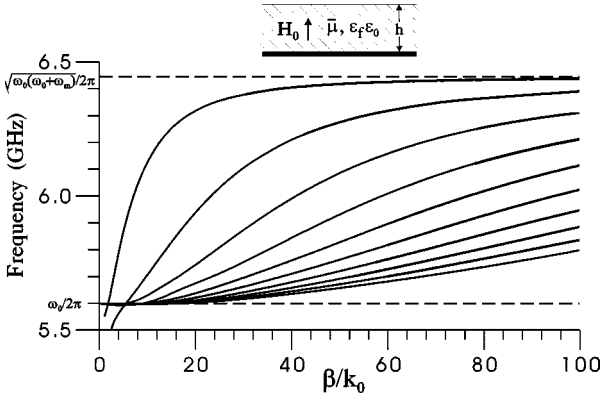

Fig. 4. Normalized phase constants (solid lines) of the magnetostatic volume-wave modes propagating along the conductor-backed ferrimagnetic slab that supports the circular microstrip patch of Fig. 3 ($h = 1.27$ mm, $\epsilon_f = 15$, $\mu_0 H_0 = 0.2$ T, $\mu_0 M_s = 0.065$ T, $\mu_0\Delta H = 0$ T).

the results obtained considering dielectric anisotropy and the results obtained neglecting dielectric anisotropy reach 2% when the anisotropic dielectric is sapphire, 3% when the dielectric is Epsilam-10, and 5% when the dielectric is boron nitride. This indicates that the errors made by ignoring dielectric anisotropy in the computation of the resonant frequencies of a microstrip patch printed on an anisotropic dielectric substrate [5] can be actually doubled when the patch is covered by an anisotropic dielectric superstrate.

In Fig. 3, results are presented for the resonant frequencies of the first five resonant modes of a circular microstrip patch printed on a magnetized ferrite. In this figure, the resonant frequencies are plotted versus the magnitude of the bias magnetic field. As in [6], [9], and [22], it is found that all resonant frequencies can be tuned over a wide frequency range by means of the bias magnetic field (in fact, when $\mu_0 H_0$ is varied from 0 to 0.4 T in Fig. 3, the resonant frequency of the resonant mode $m = -1$, $n = 1$ changes more than 100% and the resonant frequencies of the rest of the modes change more than 50% in most cases). Also, as in [10], convergent results for the resonant frequencies are not achieved in the frequency region $\mu_0\gamma H_0/2\pi < f < \mu_0\gamma\sqrt{H_0(H_0+M_s)}/2\pi$ owing to the propagation in that frequency region of an infinite number of magnetostatic volume-wave modes along the conductor-backed ferrite layer supporting the circular patch. As a consequence of the existence of this cutoff region, the resonant frequencies of all resonant modes appear below and above the cutoff region. Both the existence of a cutoff frequency region and the existence of resonances above and below the cutoff region are predicted by the cavity model (see [9, Fig. 5]). However, the cavity model fails to predict the correct limits of the cutoff region since the cavity model does not account for the propagation of magnetostatic modes [27]. This is clearly shown in Fig. 3, in which comparison is carried out between the resonant frequencies obtained for the modes $m = 1$, $n = 1$ and $m = -1$, $n = 1$ via the method of Section II, and the resonant frequencies obtained for those two modes via the cavity model. Although very good agreement is found between both sets of results for the resonant mode $m = -1$, $n = 1$ (differences are always below 7%), part of the results provided by the cavity model for the resonant mode $m = 1$, $n = 1$ are completely wrong because they lie inside the actual cutoff region. The numerical results plotted in Fig. 3 for the resonant frequencies of circular microstrip patch on a ferrite substrate closely resemble the experimental results shown in [22, Fig. 4] for the resonant frequencies of a rectangular patch on a magnetized ferrite. These experimental results seem to show the existence of a cutoff region with resonances above and below that cutoff region in spite of the fact that the theoretical model used in [22] does not predict the existence of that cutoff region. In Fig. 4, results are presented for the normalized phase constants of magnetostatic volume-wave modes propagating along the conductor-backed ferrite slab used as a substrate for the circular microstrip resonator of Fig. 3. As mentioned above, an infinite number of magnetostatic volume-wave modes are excited inside the ferrite layer in the frequency region $\omega_0/2\pi = \mu_0\gamma H_0/2\pi < f < \sqrt{\omega_0(\omega_0+\omega_m)}/2\pi = \mu_0\gamma\sqrt{H_0(H_0+M_s)}/2\pi$, which prevents resonances from occurring inside the structure of Fig. 3 in that frequency region.

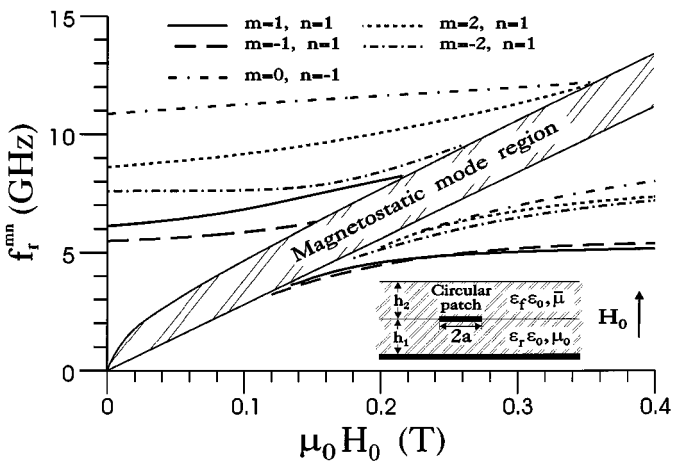

Fig. 5. Resonant frequencies of the first five resonant modes of a circular microstrip patch printed on an isotropic dielectric layer with a magnetized ferrite superstrate ($h_1 = 1.27$ mm, $h_2 = 2h_1$, $a = 5$ mm, $\epsilon_r = 2.5$, $\epsilon_f = 15$, $\mu_0 M_s = 0.178$ T, $\mu_0 \Delta H = 0.0045$ T).

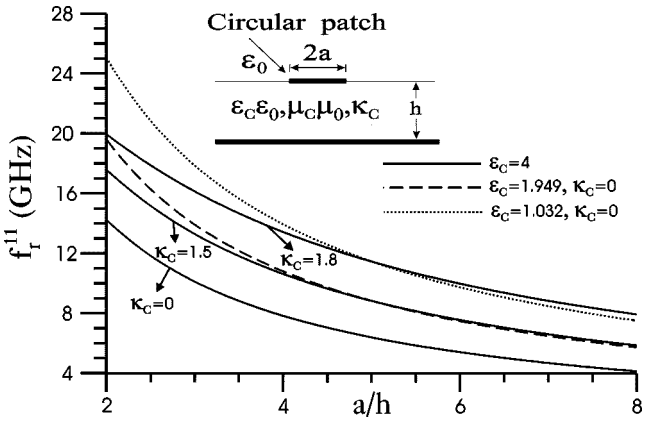

Fig. 6. Resonant frequencies of the fundamental mode ($m = 1, n = 1$) of circular microstrip patches printed on chiral materials with different values of κ_c (solid lines) and of circular microstrip patches printed on nonchiral materials (dashed and dotted lines) ($h = 1.27$ mm and $\mu_c = 1$ in all cases). The resonant frequencies of the patches on nonchiral materials with permittivities $\epsilon_c = 1.949$ and $\epsilon_c = 1.032$ coincide with those of the patches on chiral materials with $\kappa_c = 1.5$ and $\kappa_c = 1.8$, respectively, when $a/h = 5$.

The phase constants of the magnetostatic volume-wave modes have been obtained by computing the zeros of $[\tilde{\overline{\mathbf{G}}}^H_{M,M}(k_\rho)]^{-1}$ [see (7)] in the real axis of the complex k_ρ-plane (these zeros are the poles of the determinant of $\tilde{\overline{\mathbf{G}}}^H_{M,M}(k_\rho)$) [28]. Since the results plotted in Fig. 3 have been obtained for a lossless ferrite ($\Delta H = 0$), it may be thought that these results experience strong changes when ferrite losses are considered (i.e., when $\Delta H \neq 0$). However, the authors have obtained that whereas the ferrite linewidth value has a strong effect on the quality factors of the resonant modes, its effect on the resonant frequencies is negligible. Thus, in the case of the structure analyzed in Fig. 3, the authors have numerically found that as the ferrite linewidth is varied from $\mu_0 \Delta H = 0$ T to $\mu_0 \Delta H = 0.02$ T, the quality factors of the first five resonant modes are reduced to values that are at least 50% below the values in the lossless case ($\mu_0 \Delta H = 0$ T), but the resonant frequencies of the same modes (i.e., those plotted in Fig. 5) change less than 1%.

In Fig. 5, results are presented for the resonant frequencies of the first five resonant modes of a circular microstrip patch printed on a dielectric layer on top of which there is a ferrite superstrate. The figure shows that although the ferrite material does not occupy the space between the circular metallic patch and the ground plane, this material still has some effect on the resonant frequencies of the circular patch. In fact, it can be seen that as the bias field of the ferrite is varied, the resonant frequencies of the patch can be tuned over a certain frequency range. However, the width of the tuning frequency interval obtained in this case is smaller than the width of the interval that would be obtained if the ferrite were placed between the circular patch and ground plane (compare Figs. 3 and 5). Thus, when $\mu_0 H_0$ is varied from 0 to 0.4 T in Fig. 5, the changes in the resonant frequencies of most resonant modes are below 40%, and these changes in the resonant frequencies are much smaller than those observed in Fig. 3. As it happens with Fig. 3, in Fig. 5 there is a cutoff frequency region in which resonances are forbidden, and also the resonances of all resonant modes occur below the cutoff region as well as above the cutoff region. Once again, the existence of the cutoff frequency region is based on the excitation in that region of an infinite number of magnetostatic volume-wave modes along the double-layered dielectric-ferrite substrate giving support to the circular microstrip resonator analyzed in Fig. 5.

In Fig. 6, the authors plot three solid lines, which stand for the resonant frequencies of the fundamental mode of circular microstrip patches printed on chiral substrates (with $\kappa_c = 1.5$ and $\kappa_c = 1.8$) and for the resonant frequencies of the same patches printed on a nonchiral substrate of the same permittivity (for which $\kappa_c = 0$). It can be checked that the differences between the set of results obtained for the patches on chiral substrates and the set of results obtained for the patches on the nonchiral substrate with $\epsilon_c = 4$ reach 42% when $\kappa_c = 1.5$, and 93% when $\kappa_c = 1.8$. Since the resonant frequencies of the patches on chiral substrates are higher than those of the patches on a nonchiral substrate with the same permittivity, it seems that the patches on chiral substrates behave as patches printed on nonchiral substrates of lower permittivity. In order to check this statement, in Fig. 6, results are also plotted for the resonant frequencies of circular microstrip patches on two nonchiral substrates of lower permittivity (dotted and dashed lines) (the permittivity of these two substrates is computed in such a way that the resonant frequencies of the patches on chiral substrates and those of the patches on nonchiral substrates with lower permittivity coincide for $a/h = 5$). Comparison between the results obtained for patches on chiral substrates and those obtained for patches on nonchiral substrates of lower permittivity indicate that concerning the calculation of the resonant frequencies of the patches, chiral substrates are equivalent to nonchiral substrates of lower permittivity, this permittivity being slightly dependent on the geometry of the patch. Also, the permittivity of the equivalent nonchiral substrates decreases as the chiral parameter of the chiral substrates increases. In Fig. 7, results are presented for the quality factors of the fundamental resonant mode of the circular microstrip patches analyzed in Fig. 6. It can be noticed that given the value of both the radius of the patch and the thickness of the substrate, the quality factor of the patches on chiral substrates decreases as the chiral parameter

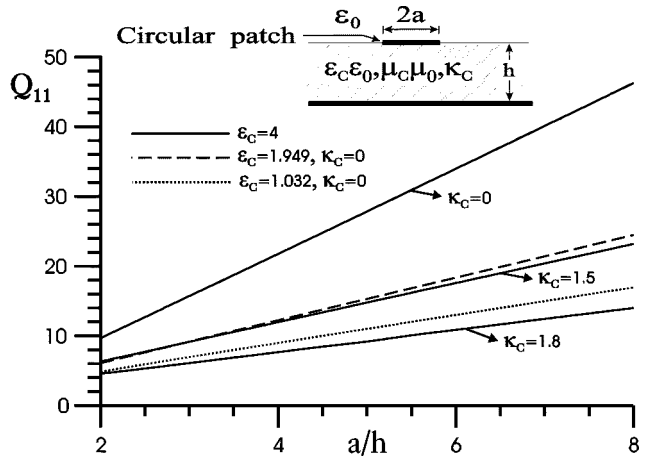

Fig. 7. Quality factors of the fundamental resonant mode ($m = 1, n = 1$) of the circular microstrip patches printed on chiral and nonchiral materials analyzed in Fig. 6 ($h = 1.27$ mm, $\mu_c = 1$).

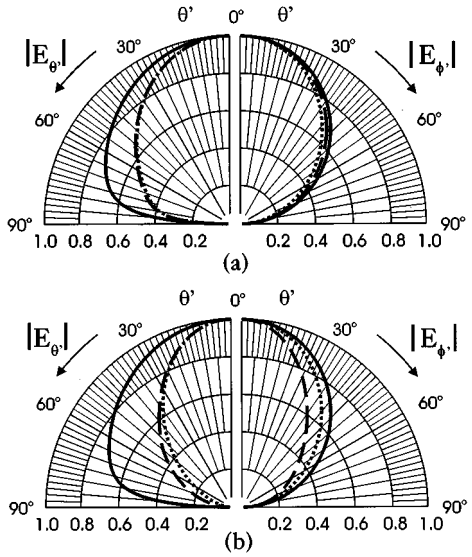

Fig. 8. Radiation patterns of the fundamental resonant mode ($m = 1, n = 1$) of circular microstrip patches printed on chiral and nonchiral materials (see Fig. 6: $h = 1.27$ mm, $a/h = 5$, $\mu_c = 1$). Solid lines stand for the results obtained when $\epsilon_c = 4$ and $\kappa_c = 0$ in (a) and (b). Dashed lines stand for the results obtained when $\epsilon_c = 4$ and $\kappa_c = 1.5$ in (a), and when $\epsilon_c = 4$ and $\kappa_c = 1.8$ in (b). Dotted lines stand for the results obtained when $\epsilon_c = 1.949$ and $\kappa_c = 0$ in (a), and when $\epsilon_c = 1.032$ and $\kappa_c = 0$ in (b).

increases. Also, the quality-factor values of the patches on chiral substrates are very close to those of the patches on equivalent nonchiral substrates of lower permittivity. Looking at Fig. 7 and taking into account that the bandwidth (inversely proportional to the quality factor) of microstrip antennas on nonchiral dielectric substrates increases as the permittivity decreases [1], it is possible to explain why the authors of [13] found that the bandwidth of microstrip antennas on chiral substrates increases as the chiral parameter increases. In Fig. 8(a) and (b), the authors plot the radiation patterns of some of the circular microstrip patches on chiral and nonchiral substrates analyzed in Fig. 6. As in Fig. 7, the results obtained in Fig. 8(a) and (b) for the patches on chiral substrates are very close to those obtained for the patches on equivalent nonchiral substrates of lower permittivity. Note that the directivity of the pattern emitted by the patches on chiral substrates increases as the chiral parameter increases, which is in agreement with the results obtained in [13] for the directivity of rectangular microstrip antennas on chiral substrates. Once again, this can be justified by the fact that the directivity of microstrip antennas printed on nonchiral dielectric substrates increases as the permittivity decreases [1].

IV. Conclusions

Galerkin's method in the HTD has been used for the numerical calculation of the resonant frequencies, quality factors, and radiation patterns of the resonant modes of circular microstrip patch resonators when the patches are embedded in a multilayered substrate that may contain uniaxial anisotropic dielectrics, magnetized ferrites, and/or chiral materials. The numerical results obtained have shown that important errors may arise in the computation of the resonant frequencies of the resonators when substrate dielectric anisotropy or substrate chirality are ignored. Also, the numerical results obtained for circular microstrip resonators on substrates containing ferrite layers have shown that the resonant frequencies of these resonators can be tuned by means of the bias magnetic field. However, it has been demonstrated that there is a cutoff frequency region for the resonant frequencies of these resonators on substrates containing ferrites owing to the excitation of an infinite number of magnetostatic volume-wave modes along the substrates of the resonators in the cutoff frequency region. Finally, the resonance and radiation properties of circular microstrip patches on chiral substrates have been explained by establishing an equivalence between the behavior of these patches and that of patches of the same size printed on nonchiral substrates of lower permittivity. This equivalence is such that the permittivity of the equivalent nonchiral substrates decreases as the chiral parameter of the chiral substrates increases.

References

[1] J. R. James and P. S. Hall, *Handbook of Microstrip Antennas*. Stevenage, U.K.: Peregrinus, 1989.
[2] K. A. Michalski and D. Zheng, "Analysis of microstrip resonators of arbitrary shape," *IEEE Trans. Microwave Theory Tech.*, vol. 40, pp. 112–119, Jan. 1992.
[3] A. Bhattacharayya and T. Tralman, "Effects of dielectric superstrate on patch antennas," *Electron. Lett.*, vol. 24, no. 6, pp. 356–358, 1988.
[4] N. G. Alexopoulos, "Integrated-circuit structures on anisotropic substrates," *IEEE Trans. Microwave Theory Tech.*, vol. MTT-33, pp. 847–881, Oct. 1985.
[5] D. M. Pozar, "Radiation and scattering from a microstrip patch on a uniaxial substrate," *IEEE Trans. Antennas Propagat.*, vol. AP-35, pp. 613–621, June 1987.
[6] D. M. Pozar and V. Sanchez, "Magnetic tuning of a microstrip antenna on a ferrite substrate," *Electron. Lett.*, vol. 24, no. 12, pp. 729–731, 1988.
[7] D. M. Pozar, "Radar cross-section of microstrip antenna on normally biased ferrite substrate," *Electron. Lett.*, vol. 25, no. 16, pp. 1079–1080, 1989.
[8] H. Y. Yang, J. A. Castaneda, and N. G. Alexopoulos, "Multifunctional and low RCS nonreciprocal microstrip antennas," *Electromag.*, vol. 12, pp. 17–31, 1992.
[9] D. M. Pozar, "Radiation and scattering characteristics of microstrip antennas on normally biased ferrite substrates," *IEEE Trans. Antennas Propagat.*, vol. 40, pp. 1084–1092, Sept. 1992.
[10] N. E. Buris, T. B. Funk, and R. S. Silverstein, "Dipole arrays printed on ferrite substrates," *IEEE Trans. Antennas Propagat.*, vol. 41, pp. 165–175, Feb. 1993.

[11] I. V. Lindell, A. H. Sihvola, S. A. Tretyskov, and A. J. Vitanen, *Electromagnetic Waves in Chiral and Bi-isotropic Media*. Norwood, MA: Artech House, 1994.
[12] D. M. Pozar, "Microstrip antennas and arrays on chiral substrates," *IEEE Trans. Antennas Propagat.*, vol. 40, pp. 1260–1263, Oct. 1992.
[13] A. Toscano and L. Vegni, "A new efficient moment method formulation for the design of microstrip antennas over a chiral grounded slab," *J. Electromag. Waves Applicat.*, vol. 11, no. 5, pp. 567–592, 1997.
[14] W. C. Chew and J. A. Kong, "Resonance of the axial-symmetric modes in microstrip disk resonators," *J. Math. Phys.*, vol. 21, pp. 582–591, Mar. 1980.
[15] ——, "Resonance of nonaxial symmetric modes in circular microstrip disk antenna," *J. Math. Phys.*, vol. 21, pp. 2590–2598, Oct. 1980.
[16] K. Araki and T. Itoh, "Hankel transform domain analysis of open circular microstrip radiating structures," *IEEE Trans. Antennas Propagat.*, vol. AP-29, pp. 84–89, Jan. 1981.
[17] R. M. Nelson, D. A. Rogers, and A. G. D'Assuncao, "Resonant frequency of a rectangular microstrip patch on several uniaxial substrates," *IEEE Trans. Antennas Propagat.*, vol. AP-38, pp. 973–981, July 1990.
[18] T. Q. Ho, B. Beker, Y. C. Shih, and Y. Chen, "Microstrip resonators on anisotropic substrates," *IEEE Trans. Microwave Theory Tech.*, vol. 40, pp. 762–765, Apr. 1992.
[19] K. L. Wong, J. S. Row, C. W. Kuo, and K. C. Huang, "Resonance of a rectangular microstrip patch on a uniaxial substrate," *IEEE Trans. Microwave Theory Tech.*, vol. 41, pp. 698–701, Apr. 1993.
[20] Z. Cai and J. Bornemann, "Rigorous analysis of radiation properties of lossy patch resonators on complex anisotropic media and lossy ground metallization," *IEEE Trans. Antennas Propagat.*, vol. 42, pp. 1443–1446, Oct. 1994.
[21] K. Araki, D. I. Kim, and Y. Naito, "A study on circular disk resonators on a ferrite substrate," *IEEE Trans. Microwave Theory Tech.*, vol. MTT-30, pp. 147–154, Feb. 1982.
[22] H. How, T. M. Fang, and C. Vittoria, "Intrinsic modes of radiation in ferrite patch antennas," *IEEE Trans. Microwave Theory Tech.*, vol. 42, pp. 988–994, June 1994.
[23] D. M. Pozar, *Microwave Engineering*. Reading, MA: Addison-Wesley, 1990.
[24] V. Losada, R. R. Boix, and M. Horno, "Resonant modes of circular microstrip patches in multilayered substrates," *IEEE Trans. Microwave Theory Tech.*, vol. 47, pp. 488–498, Apr. 1999.
[25] F. L. Mesa, R. Marques, and M. Horno, "A general algorithm for computing the bidimensional spectral Green's dyad in multilayered complex bianisotropic media: The equivalent boundary method," *IEEE Trans. Microwave Theory Tech.*, vol. 39, pp. 1640–1649, Sept. 1991.
[26] R. E. Colin, *Antennas and Radiowave Propagation*. New York: McGraw-Hill, 1985.
[27] V. Losada, R. R. Boix, and M. Horno, "Analysis of circular stripline resonators on normally biased ferrite substrates," *IEEE Microwave Guided Wave Lett.*, vol. 8, pp. 226–228, June 1998.
[28] R. R. Boix, N. G. Alexopoulos, and M. Horno, "Efficient numerical computation of the spectral traverse dyadic Green's function in stratified anisotropic media," *J. Electromag. Waves Applicat.*, vol. 10, no. 8, pp. 1047–1083, 1996.

Vicente Losada was born in São Paulo, Brazil, in 1969. He received the Licenciado and Doctor degrees in physics from the University of Seville, Seville, Spain, in 1992 and 1997, respectively.

In 1999, he became an Assistant Professor in the Department of Applied Physics, University of Seville. His research activities are currently focused on the analysis of circular microstrip resonators and antennas embedded in multilayered substrates containing complex substrates (e.g., anisotropic dielectrics, ferrites, chiral media).

Rafael R. Boix (M'97) was born in Melilla, Spain, in 1962. He received the Licenciado and Doctor degrees in physics from the University of Seville, Seville, Spain, in 1985 and 1990 respectively.

Since 1985, he has been with the Electronics and Electromagnetics Department, University of Seville, where he became an Associate Professor in 1994. During the summers of 1991 and 1992, he was with the Electrical Engineering Department, University of California at Los Angeles (UCLA), as a Visiting Scholar. During the summer of 1996, he was with the Electrical and Computer Engineering Department, Syracuse University, Syracuse, NY, as a Visiting Scholar. His current research interest is focused on the analysis of the effects of complex substrates on the performance of planar transmission-line discontinuities, planar passive microwave circuits, planar resonators, and PCA's.

Manuel Horno (M'75) was born in Torre del Campo, Jaen, Spain, in 1947, and died in September 1998, in Seville, Spain. He received the Licenciado and Doctor degrees in physics from the University of Seville, Seville, Spain, in 1969 and 1972 respectively. In 1969, he joined the Department of Electronics and Electromagnetics, University of Seville, where he became Associate Professor in 1975 and Full Professor in 1986. His research was focused on the solution of boundary value problems in electromagnetic theory, wave propagation through anisotropic media and MIC's. During his final years, he was engaged in the analysis of planar transmission lines embedded in complex materials, synthesis of passive microwave circuits containing planar transmission lines, and characterization of planar transmission-line discontinuities and printed antennas.

Prof. Horno was a member of the Electromagnetic Academy, Massachusetts Institute of Technology (MIT), Cambridge.